Supporting information

From Sequential Molecular Adsorption on Atomically Precise Ag_{29} Nanoclusters to Aggregates of Soot-Like Particles

Jayoti Roy,[†,‡] Marco Neumaier,[‡,§] Christoph Plett,[⊥] Papri Chakraborty,[‡,§,∥] Anirban Som,[†] Arijit Jana,[†] Stefan Grimme,[⊥] Horst Hahn,[#] Manfred M. Kappes,*[,‡,§] and Thalappil Pradeep*[,†,¶]

[†]DST Unit of Nanoscience (DST UNS) & Thematic Unit of Excellence (TUE), Department of Chemistry, Indian Institute of Technology Madras, Chennai 600036, India.

[‡]Institute of Physical Chemistry, Karlsruhe Institute of Technology (KIT), Kaiserstr. 12, 76131 Karlsruhe, Germany.

[§]Institute of Nanotechnology, Karlsruhe Institute of Technology (KIT), Kaiserstr. 12, 76131, Karlsruhe, Germany.

[∥]Institute for Quantum Materials and Technologies, Karlsruhe Institute of Technology (KIT), Kaiserstr. 12, 76131, Karlsruhe, Germany.

[⊥]Mulliken Center for Theoretical Chemistry, Clausius-Institut für Physikalische und Theoretische Chemie, Universität Bonn, Beringstraße 4, 53115 Bonn, Germany.

[#]Department of Materials Science and Engineering, The University of Arizona, 1235 James E. Rogers Way, Tucson, AZ 85719, United States.

[¶]International Centre for Clean Water, 2nd Floor, B-Block, IIT Madras Research Park, Kanagam Road, Taramani, Chennai 600113, India.

*Email: manfred.kappes@kit.edu.

*Email: pradeep@iitm.ac.in. Fax: 91-44-2257-0545/0509.

This PDF file includes:

Experimental Section

SI1.1 Reagents and Materials

All the chemicals, excluding NCs and **R1**S_2H_2, were commercially available and employed without further purification. Silver nitrate ($AgNO_3$, 99.9%) was procured from Rankem, India. Sodium borohydride ($NaBH_4$), 1,3-benzene dithiol (1,3-BDT), benzene-1,4-dicarbaldehyde, and ortho-aminothiophenol were obtained from Sigma-Aldrich. Triphenylphosphine (PPh_3) was purchased from Spectrochem, India. All the solvents, methanol (MeOH), dimethylformamide (DMF), acetonitrile, and ethanol (EtOH) were of the HPLC grade (≥ 99.9%) and used without further purification.

SI1.2 Synthesis

SI1.2.1 Synthesis of $[Ag_{29}(BDT)_{12}(PPh_3)_4]$ nanocluster

$[Ag_{29}(BDT)_{12}(PPh_3)_4]$ cluster was synthesized following the reported method with slight modification.[1] About 20 mg of $AgNO_3$ was dissolved in a mixture of 5 mL MeOH and 7 mL of DCM. About 13.5 μL of BDT ligand was then added to the reaction mixture. Due to Ag-S complex formation upon addition of the thiol, the color of the solution turned yellow. The mixture was kept under stirring condition and shortly after this, 200 mg of PPh_3 dissolved in 1 mL of DCM was added. This addition led to a transition in the color of the solution from yellow to colorless, signifying the development of Ag-S-P complexes. After ~15 min, 10.5 mg of $NaBH_4$ dissolved in 0.5 mL of water was added. After the addition of $NaBH_4$, the solution immediately turned a dark brown color, which further changed to orange gradually indicating the formation of the nanoclusters. The entire reaction was carried out under dark conditions to avoid oxidation of silver. After 4 h of continuous stirring in the dark, the reaction mixture was centrifuged and the supernatant was discarded. The dark brown precipitate was washed repeatedly with ethanol to remove all of the unreacted compounds and complexes to get a purified nanocluster, which was further dried using rotavapor to obtain a powder.[1,17]

SI1.2.2 Synthesis of secondary ligand -2,2′-[1,4-Phenylenebis(methylidynenitrilo)] bis[benzenethiol (**R1**S_2H_2)

The **R1**S_2H_2 secondary ligand was synthesized through a thermal condensation reaction following an earlier report.[18] In brief, ~500 mg (~3.5 mM) of benzene-1,4-dicarbaldehyde was dissolved in EtOH. ~1.125 g (~9 mM) ortho-aminothiophenol was also dissolved in MeOH-EtOH (2:1, v/v) solvent mixture. It was added dropwise to the solution at inert argon closed condition, which resulted in some yellow precipitates. As-synthesized yellow precipitates are kept for 1 day under reflux conditions. Recrystallized sample from hot DCM/hexane mixture was used for further studies. The yield of the product is 85 %. The product was soluble in various organic solvents such as DMF, DCM, MeOH, and acetonitrile.

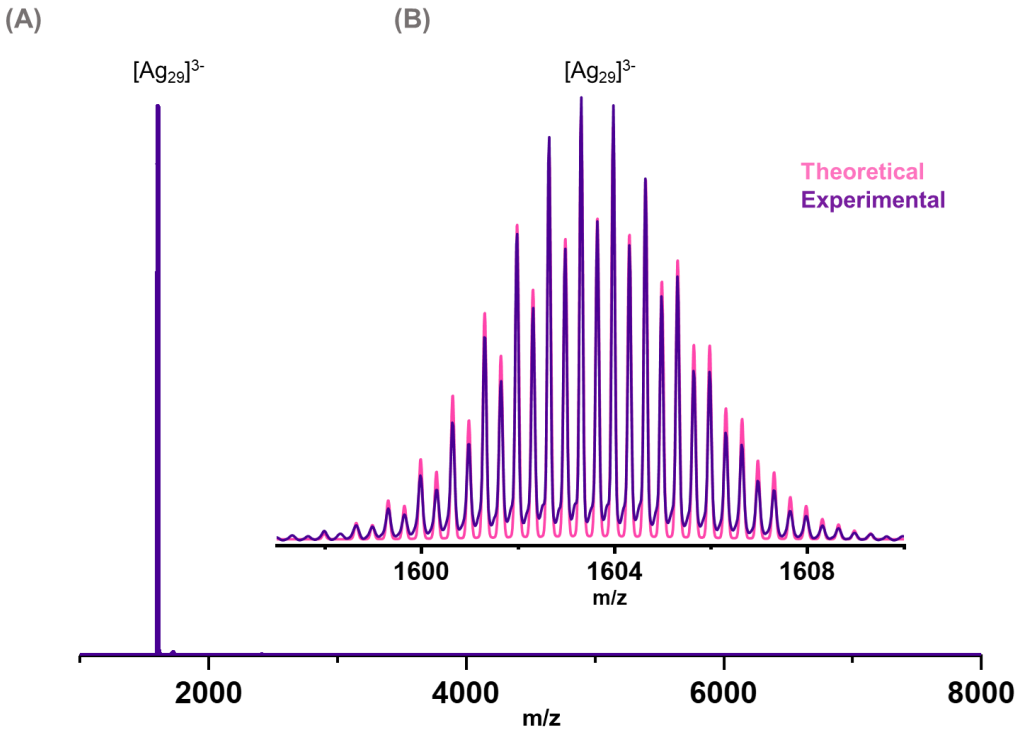

Figure S1.(A) Negative mode full range ESI MS of $[Ag_{29}]^{3-}$. (B) Overlapped isotopic distributions of experimental (color: Purple) $[Ag_{29}]^{3-}$ with theoretically (color: Pink) calculated one.

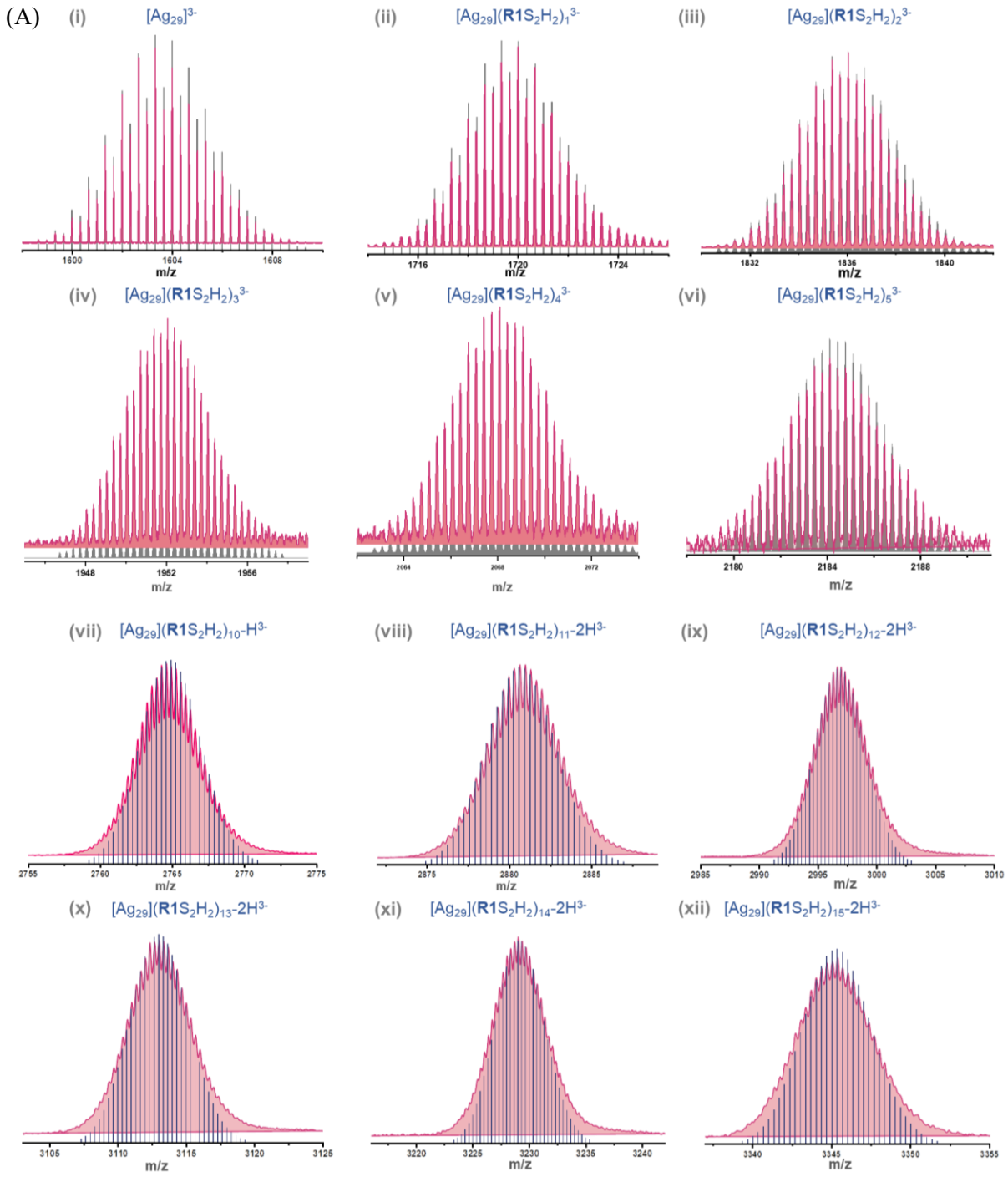

Figure S2.(A) Experimental and theoretical isotopic distribution of (i) $[Ag_{29}]^{3-}$ NC without **R1**S_2H_2, and (ii)-(xii) $[Ag_{29}](\mathbf{R1}S_2H_2)_n^{3-}$, respectively $\{[Ag_{29}](\mathbf{R1}S_2H_2)_n\text{-}xH\}^{3-}$, adducts with *n* and *x* as indicated. Peaks in vivid pink and dark gray represent the experimental and theoretical isotopic distribution, respectively. Partial ESI-MS correspond to a $[Ag_{29}]^{3-}$:**R1**S_2H_2 (0.14) solution in acetonitrile sampled within 60 s of mixing.

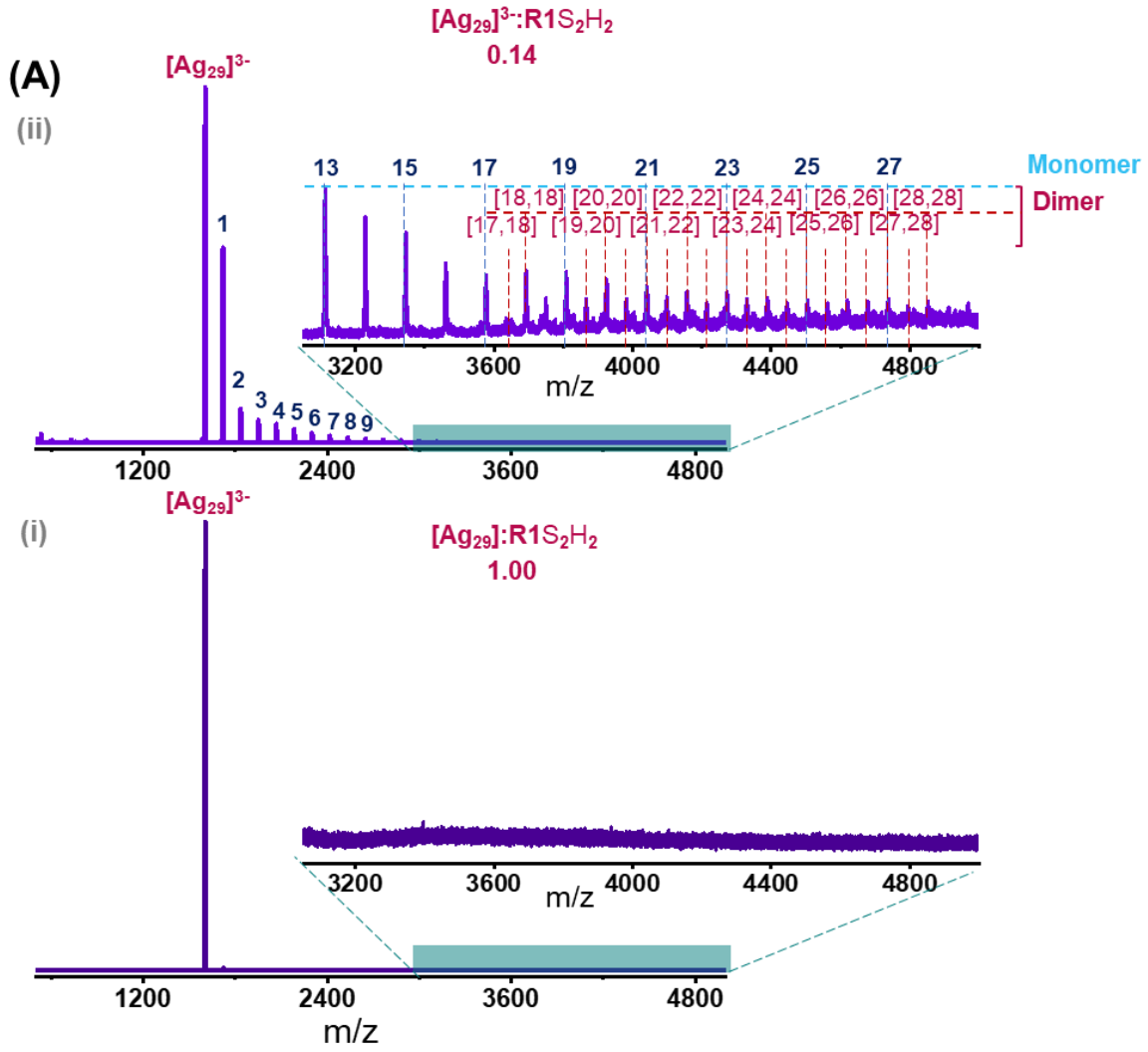

Figure S3.(A) Full range negative mode ESI MS spectra of (i) $[Ag_{29}]^{3-}$ solution without additional ligand **R1**S_2H_2 and (ii) $[Ag_{29}]^{3-}$:**R1**S_2H_2 (0.14) solution (60 s after mixing). Inset (i) shows no additional peaks at m/z range 3100-5000. Inset (ii) shows the NC-**R1**S_2H_2 adduct ions as monomers and dimers.

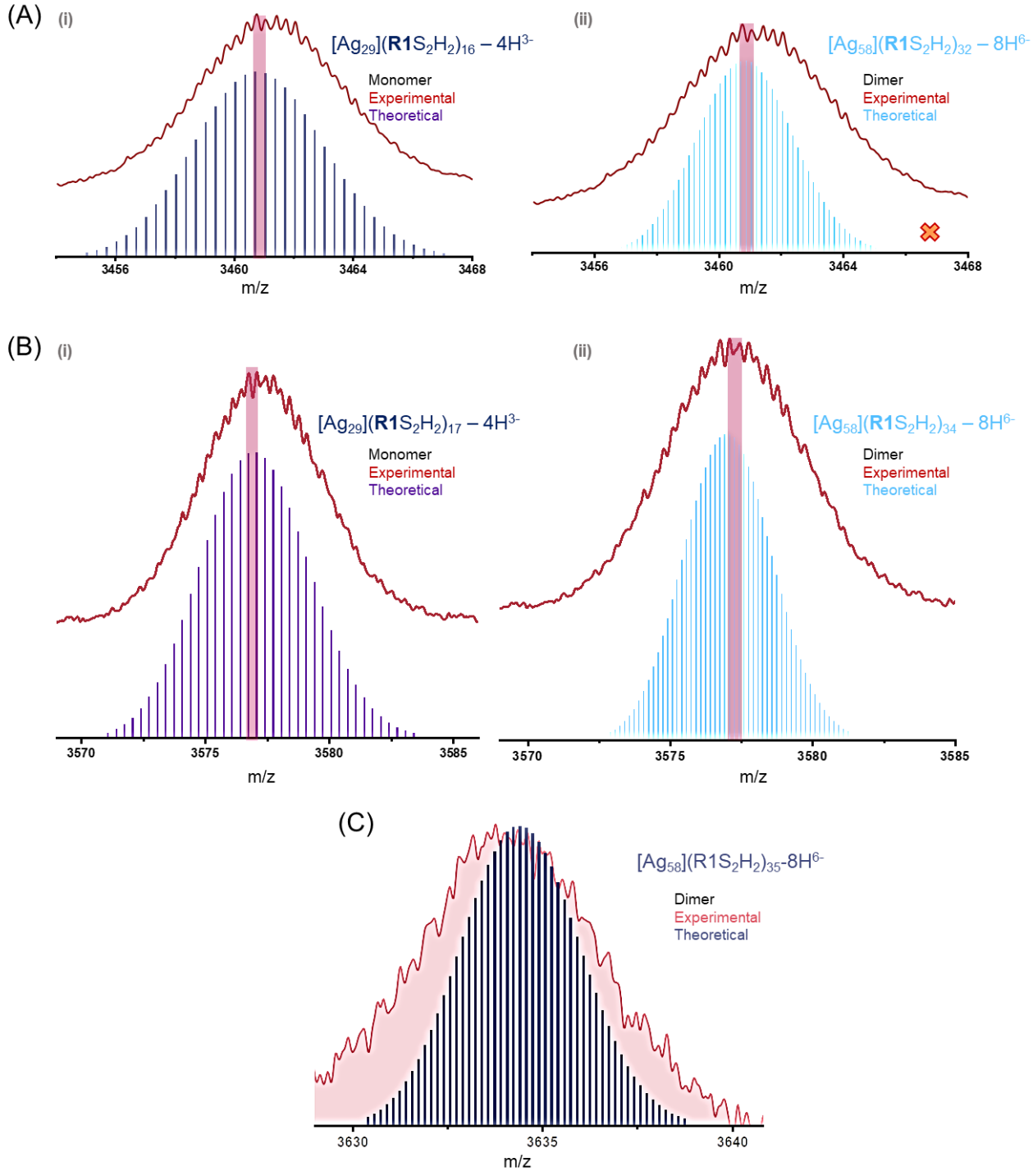

Figure S4. (A) Theoretically calculated isotopic distribution of $[Ag_{29}](\mathbf{R1}S_2H_2)_{16}$ -xH$\}^{3-}$ - monomer (i), and $\{[Ag_{58}](\mathbf{R1}S_2H_2)_{32}$-$yH\}^{6-}$ dimer (ii) under the assumption of given x and y as indicated, matched with experimental peak distribution. Cross symbol (×) denotes the theoretical isotopic distribution, highlighting its mismatch with the experimentally observed isotopic pattern. (B) Theoretically calculated isotopic distribution of $\{[Ag_{29}](\mathbf{R1}S_2H_2)_{17}$-$xH\}^{3-}$ monomer (i), and $\{[Ag_{58}](\mathbf{R1}S_2H_2)_{34}$-$yH\}^{6-}$ (17,17) dimer (ii), well-matched with experimental peak distribution. (C) Isotopic distribution of the (17,18) dimer along with its theoretically calculated distribution. Calculated isotopic distribution of monomers with the assumption of $x = 4$ shows slight shifts in the overlay plot, while the experimental distribution suggests that x may differ from, but remain close to, 4.

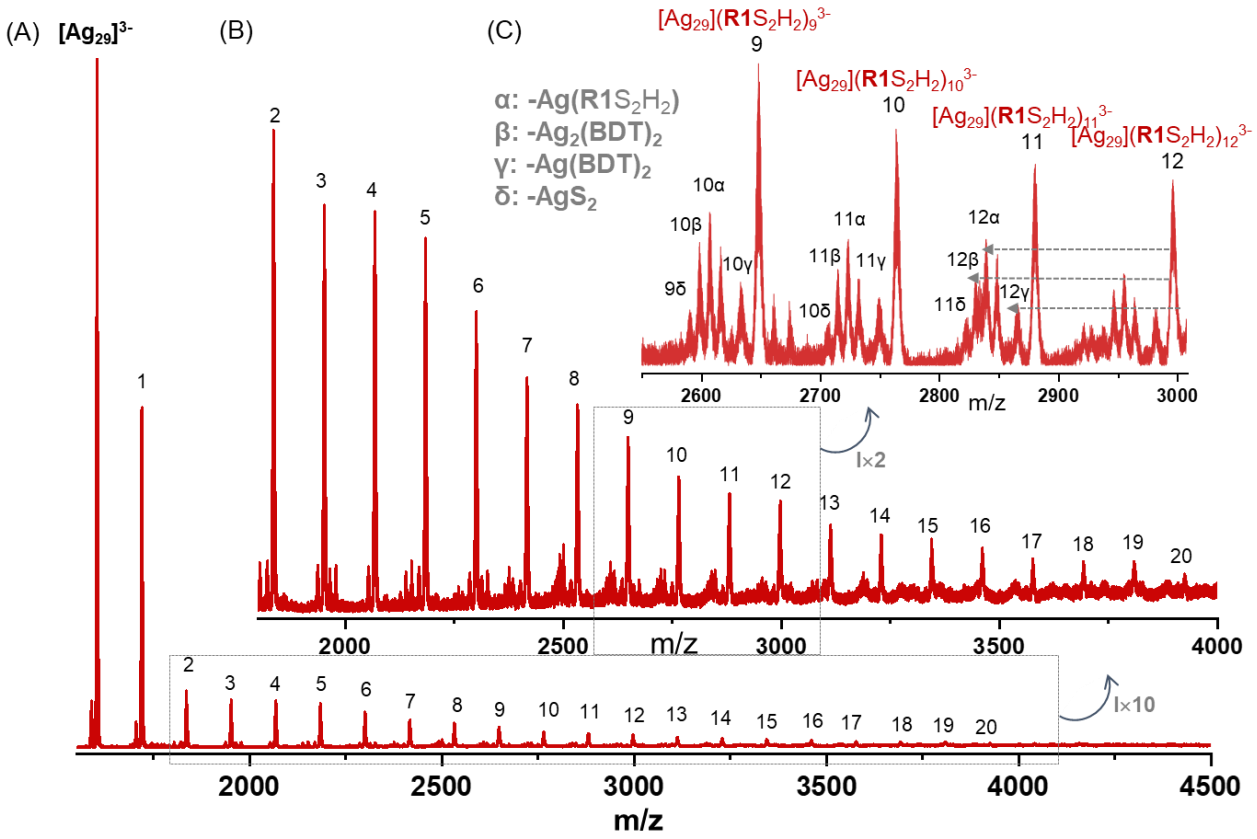

Figure S5. (A) Full range ESI MS recorded within 60 s after mixing for a molar ratio of 0.02 of $[Ag_{29}]$:**R1**S_2H_2. (B-C) show the expanded ESI MS of (A). I corresponds to the Zoom factors. The intermediate peaks between $[Ag_{29}](\mathbf{R1}S_2H_2)_n^{3-}$ adducts are labelled with nα, nβ, nγ, nδ indicating fragmentation. n is the nominal number of **R1**S_2H_2 ligands in $[Ag_{29}](\mathbf{R1}S_2H_2)_n^{3-}$.

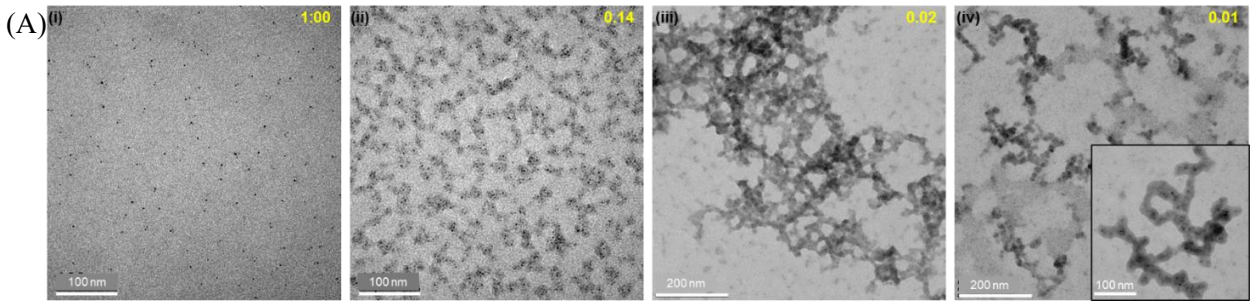

Figure S6.(A) HRTEM micrographs of (i) $[Ag_{29}]^{3-}$ NC, (ii) $[Ag_{29}]^{3-}$:**R1**S_2H_2 (0.14), (iii) $[Ag_{29}]^{3-}$:**R1**S_2H_2 (0.02), and (iv) $[Ag_{29}]^{3-}$:**R1**S_2H_2 (0.01) solutions (after drop coating the respective solutions onto TEM grids). Values in parentheses indicate the ratios of $[Ag_{29}]^{3-}$:**R1**S_2H_2 in solution.

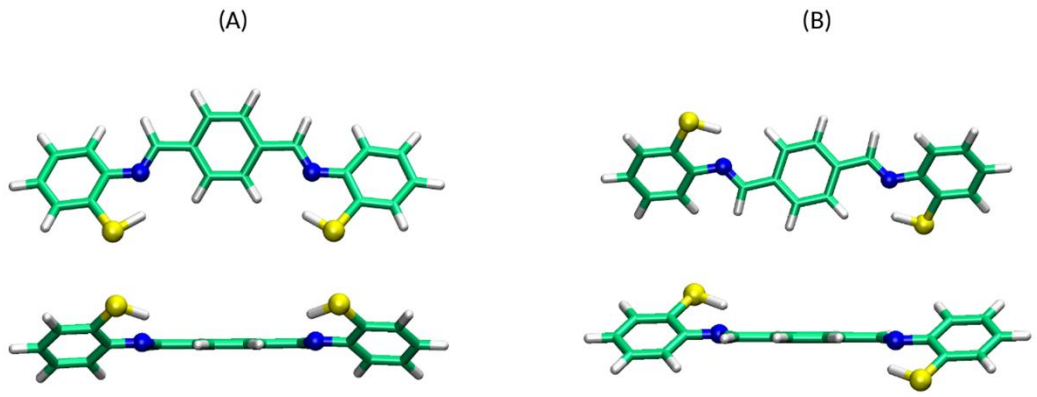

Figure S7. GFN2 xTB structures of the ligand **R1**S_2H_2 in (A) *cis* and (B) *trans* configuration.

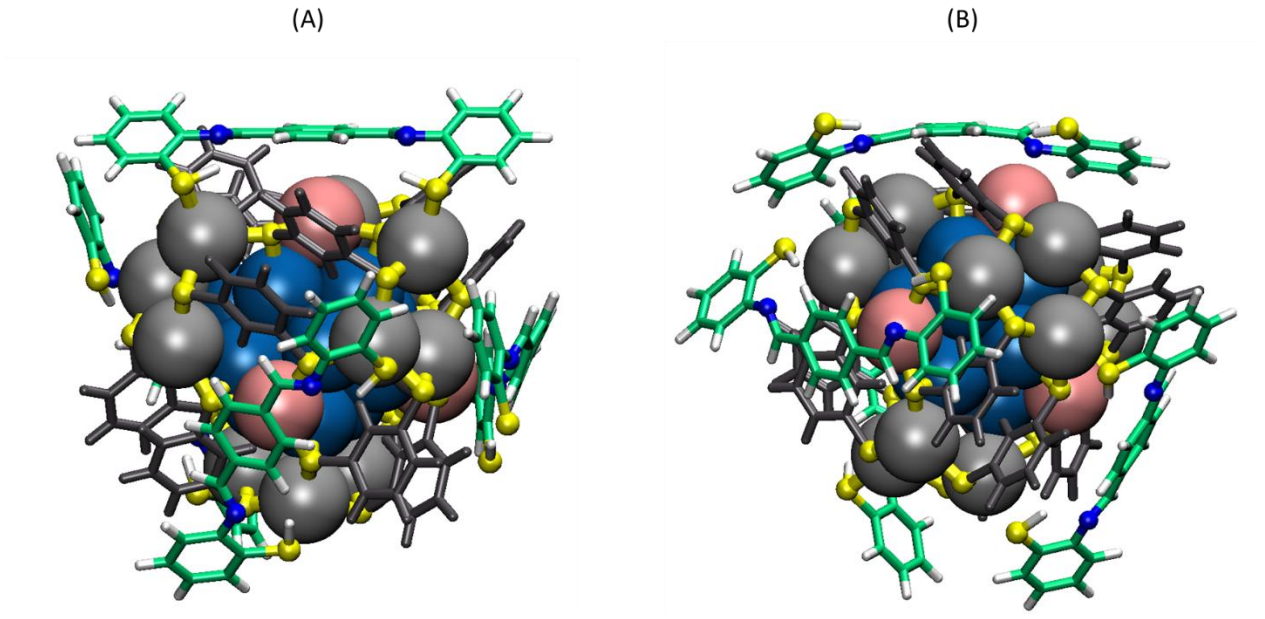

Figure S8. Structure of $[Ag_{29}](\mathbf{R1}S_2H_2)_4^{3-}$ as received from aISS docking shown for two different orientations (A-B). Color code: ^{i}Ag (icosahedron Ag) – dark prussian blue; ^{t}Ag (tetrahedral Ag) – pink; ^{c}Ag (crown Ag) – grey, C and H of the BDT ligands of $[Ag_{29}]^{3-}$ – dark gray; C of **R1**S_2H_2 – light green; S – yellow; H of **R1**S_2H_2 – light gray and N - blue.

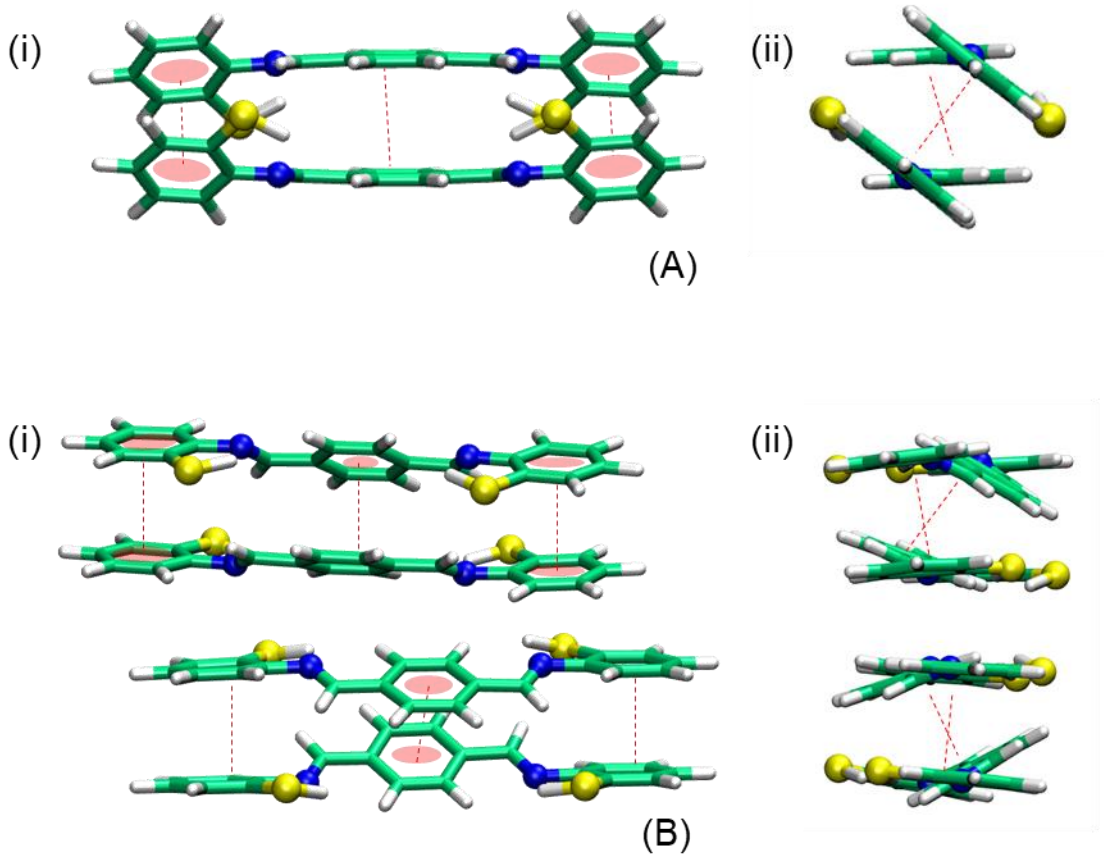

Figure S9. GFN1-xTB structures of a ligand dimer (**R1**$S_2H_2)_2$ (A), and a tetramer (**R1**$S_2H_2)_4$ (B) from aISS docking. The latter was calculated by docking two (**R1**$S_2H_2)_2$ dimers.

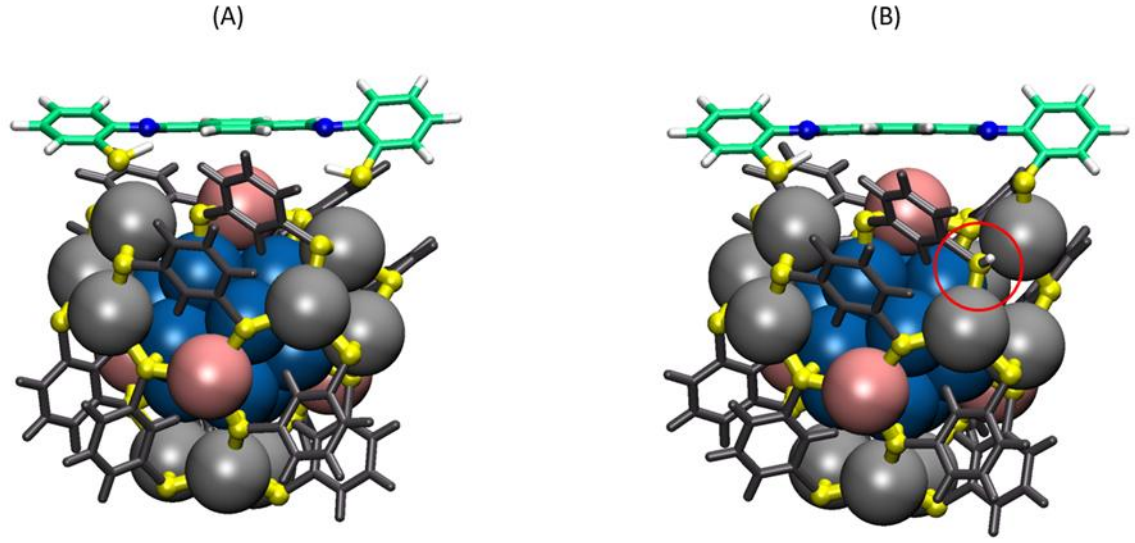

Figure S10. (A) DFT optimized structure of $[Ag_{29}]$(**R1**$S_2H_2)^{3-}$ with one "tangentially" oriented, physisorbed ligand. (B) DFT optimized structure of $\{[Ag_{29}]$(**R1**$S_2H_1)$+$H\}^{3-}$ where the H^+ of the ligand was transferred from the right -SH group to a BDT S-atom (see red circle).

References

(1) G. AbdulHalim, L.; S. Bootharaju, M.; Tang, Q.; Del Gobbo, S.; G. AbdulHalim, R.; Eddaoudi, M.; Jiang, D.; M. Bakr, O.; AbdulHalim, L. G.; Bootharaju, M. S.; Tang, Q.; Gobbo, S. Del; AbdulHalim, R. G.; Eddaoudi, M.; Jiang, D.; Bakr, O. M. $Ag_{29}(BDT)_{12}(TPP)_4$: A Tetravalent Nanocluster. *Journal of the American Chemical Society* **2015**, *137* (37), 11970–11975. https://doi.org/10.1021/JACS.5B04547.

(2) Plett, C.; Grimme, S. Automated and Efficient Generation of General Molecular Aggregate Structures. *Angewandte Chemie - International Edition* **2023**, *62* (4). https://doi.org/10.1002/anie.202214477.

(3) Grimme, S.; Bannwarth, C.; Shushkov, P. A Robust and Accurate Tight-Binding Quantum Chemical Method for Structures, Vibrational Frequencies, and Noncovalent Interactions of Large Molecular Systems Parametrized for All Spd-Block Elements (Z = 1-86). *Journal of Chemical Theory and Computation* **2017**, *13* (5), 1989–2009. https://doi.org/10.1021/acs.jctc.7b00118.

(4) Pracht, P.; Bohle, F.; Grimme, S. Automated Exploration of the Low-Energy Chemical Space with Fast Quantum Chemical Methods. *Physical Chemistry Chemical Physics* **2020**, *22* (14), 7169–7192. https://doi.org/10.1039/c9cp06869d.

(5) Bannwarth, C.; Ehlert, S.; Grimme, S. GFN2-XTB - An Accurate and Broadly Parametrized Self-Consistent Tight-Binding Quantum Chemical Method with Multipole Electrostatics and Density-Dependent Dispersion Contributions. *Journal of Chemical Theory and Computation* **2019**, *15* (3), 1652–1671. https://doi.org/10.1021/acs.jctc.8b01176.

(6) Ehlert, S.; Stahn, M.; Spicher, S.; Grimme, S. Robust and Efficient Implicit Solvation Model for Fast Semiempirical Methods. *Journal of Chemical Theory and Computation* **2021**, *17* (7), 4250–4261. https://doi.org/10.1021/acs.jctc.1c00471.

(7) Grimme, S.; Bohle, F.; Hansen, A.; Pracht, P.; Spicher, S.; Stahn, M. Efficient Quantum Chemical Calculation of Structure Ensembles and Free Energies for Nonrigid Molecules. *Journal of Physical Chemistry A* **2021**, *125* (19), 4039–4054. https://doi.org/10.1021/acs.jpca.1c00971.

(8) Grimme, S.; Hansen, A.; Ehlert, S.; Mewes, J. M. R2SCAN-3c: A "Swiss Army Knife" Composite Electronic-Structure Method. *Journal of Chemical Physics* **2021**, *154* (6). https://doi.org/10.1063/5.0040021.

(9) Klamt, A. Conductor-like Screening Model for Real Solvents: A New Approach to the Quantitative Calculation of Solvation Phenomena. *Journal of Physical Chemistry* **1995**, *99* (7), 2224–2235. https://doi.org/10.1021/j100007a062.

(10) Ahlrichs, R.; Bär, M.; Häser, M.; Horn, H.; Kölmel, C. Electronic Structure Calculations on Workstation Computers: The Program System Turbomole. *Chemical Physics Letters* **1989**, *162* (3), 165–169. https://doi.org/10.1016/0009-2614(89)85118-8.

(11) Perdew, J. P. Erratum: Density-Functional Approximation for the Correlation Energy of the Inhomogeneous Electron Gas. *Physical Review B* **1986**, *34* (10), 7406–7406. https://doi.org/10.1103/PhysRevB.34.7406.

(12) Becke, A. D. Density-Functional Exchange-Energy Approximation with Correct Asymptotic Behavior. *Physical Review A* **1988**, *38* (6), 3098. https://doi.org/10.1103/PhysRevA.38.3098.

(13) Kassel, L. S. The Limiting High Temperature Rotational Partition Function of Nonrigid Molecules: I. General Theory. II. CH_4, C_2H_6, C_3H_8, $CH(CH_3)_3$, $C(CH_3)_4$ and $CH_3(CH_2)_2CH_3$. III. Benzene and Its Eleven Methyl Derivatives. *The Journal of Chemical Physics* **1936**, *4* (4), 276–282. https://doi.org/10.1063/1.1749835.

(14) Mardirossian, N.; Head-Gordon, M. ΩB97X-V: A 10-Parameter, Range-Separated Hybrid, Generalized Gradient Approximation Density Functional with Nonlocal Correlation, Designed by a Survival-of-the-Fittest Strategy. *Physical Chemistry Chemical Physics* **2014**, *16* (21), 9904–9924. https://doi.org/10.1039/C3CP54374A.

(15) Weigend, F.; Ahlrichs, R. Balanced Basis Sets of Split Valence, Triple Zeta Valence and Quadruple Zeta Valence Quality for H to Rn: Design and Assessment of Accuracy. *Physical Chemistry Chemical Physics* **2005**, *7* (18), 3297. https://doi.org/10.1039/b508541a.

(16) Neese, F. The ORCA Program System. *Wiley Interdisciplinary Reviews: Computational Molecular Science* **2012**, *2* (1), 73–78. https://doi.org/10.1002/wcms.81.

(17) Nag, A.; Chakraborty, P.; Paramasivam, G.; Bodiuzzaman, M.; Natarajan, G.; Pradeep, T. Isomerism in Supramolecular Adducts of Atomically Precise Nanoparticles. *Journal of the American Chemical Society* **2018**, *140* (42), 13590–13593. https://doi.org/10.1021/JACS.8B08767.

(18) Wang, X.; Li, G.; Li, X.; Zhu, D.; Shen, R. One-Pot Three-Component Reaction of p-Quinone Monoacetals, L-Proline and Naphthols to Afford N-Aryl-2-Arylpyrrolidines. *Organic Chemistry Frontiers* **2021**, *8* (2), 297–303. https://doi.org/10.1039/D0QO01294G.